Calcif Tissue Int (2008) 83:70–79
DOI 10.1007/s00223-008-9150-5

The Magnitude and Rate of Bone Loss in Ovariectomized Mice Differs Among Inbred Strains as Determined by Longitudinal In vivo Micro-Computed Tomography

Josh Klinck · Steven K. Boyd

Received: 14 December 2007 / Accepted: 7 May 2008 / Published online: 26 June 2008

Abstract Osteoporosis is characterized by low bone mass and a deterioration of bone architecture and likely is influenced by genetic factors. The ovariectomized (OVX) mouse is well suited for osteoporosis research, as shown to date by cross-sectional studies. Here, we investigate longitudinal changes by in vivo micro-computed tomography (micro-CT) to examine the skeletal response to OVX and patterns of change in three inbred strains of mice. We address whether higher baseline bone mass among the strains of mice provides protection against bone loss and if there is a common base level of bone quantity despite genetic background after the effects of OVX have stabilized. Groups of mice ($n = 7$ or 8/group) from three inbred strains (C3H/HeJ, C57BL/6J, BALB/cByJ) were subjected to OVX or sham OVX surgery at 12 weeks of age. Weekly in vivo micro-CT scans were performed for 5 weeks at the proximal tibia (skipping week 4). Femurs were harvested after week 5 for analysis of the distal metaphysis and midshaft. The baseline bone architecture differed among the three inbred strains of mice, as did the longitudinal patterns of change due to OVX. At the end point, all three strains retained different bone architecture at the proximal tibia, distal femur, and femur midshaft. Rate of bone loss was correlated to amount of baseline bone volume ($R = 0.82$, $P < 0.001$). Morphological analysis indicated that trabecular bone loss due to OVX was manifested through reduced connectivity instead of overall thinning and that the quantity and rate of bone loss due to estrogen deficiency were in part genetically regulated.

Keywords In vivo micro-CT · Ovariectomy · Mouse · Bone architecture · Bone loss · Tibia · Femur

Osteoporosis leads to increased fracture risk as a result of reduced bone mass and decreased architectural integrity. Osteoporotic fractures occur frequently within elderly populations and have a significant impact on morbidity and mortality [1, 2]. The economic impact associated with treating such fractures places a critical burden on health-care systems [3]. Bone loss in women is predominantly associated with estrogen loss that occurs during and after menopause; however, there is large variation among patient populations in the rate and extent to which bone loss occurs [4–6]. It has been suggested that genetic factors may play a role in individual susceptibility to estrogen deficiency–related bone loss [4–8].

Studying genetic factors relating to osteoporosis in humans is difficult because of the tremendous population variance and the fact that changes occur over several years. The ovariectomized (OVX) mouse has grown in interest as an animal model for studies of estrogen-deficient bone loss because of the complete mapping of the mouse genome and the availability of inbred strains with widely varying structural and biomechanical properties [9–11]. OVX surgery in mice can result in significant bone loss within a number of weeks [12, 13], and past studies have observed differences between mouse strains in the skeletal response

J. Klinck · S. K. Boyd
Department of Mechanical and Manufacturing Engineering, University of Calgary, Calgary, Canada

J. Klinck · S. K. Boyd
Roger Jackson Centre for Health and Wellness Research, University of Calgary, Calgary, Canada

S. K. Boyd (✉)
Schulich School of Engineering, University of Calgary, 2500 University Drive NW, Calgary, Alberta, Canada T2N 1N4
e-mail: skboyd@ucalgary.ca

to OVX, supporting the hypothesis that skeletal response to estrogen deficiency is genetically regulated in mice [13, 14]. Ex vivo cross-sectional studies provide important insight into OVX-related bone loss, and longitudinal measurements by in vivo analysis can provide additional information about the temporal trends of those changes [15], provided that radiation effects due to repeated micro-computed tomographic (CT) scans are carefully considered [16, 17]. The longitudinal data provide an opportunity to address whether baseline bone mass is a determinant of the rate of bone loss and if a high bone mass protects against osteoporotic progression. Using temporal data, we addressed whether there is a common asymptote of bone quantity following OVX that is independent of genetic background.

The purpose of this study was to characterize the temporal patterns of bone loss among three commonly used genetic mouse strains and to determine if the magnitude and rate of bone loss are dependent on baseline bone quantity. This study monitored in vivo bone morphology at the proximal tibia and end point morphology at the distal femur and midshaft in mice that underwent sham surgery and OVX.

Methods

Micro-CT Scanning

Female mice from three commonly utilized inbred strains (C3H/HeJ [C3H], C57BL/6J [B6], BALB/cByJ [BALB]) were subjected to OVX ($n = 7$ or 8 per strain) or sham OVX ($n = 7$ or 8 per strain) surgery at 12 weeks of age. The mice were maintained in an accredited animal care facility at room temperature under a 12-hour light/dark cycle and provided with sterile food (Lab Mouse Diet 5062 [protein 21.8%, fat 9.0%, mineral 5.0%; Ca:P ratio 0.87]; Purina Mills, St. Louis, MO) and filtered water ad libitum.

An in vivo micro-CT scanner (vivaCT 40; Scanco Medical, Bassersdorf, Switzerland) was used to perform measurements at the proximal tibia. Animals were under anesthesia (1.75% v/v isoflurane) and secured in the scanner with a custom leg holder [15], which allowed scanning tomographic slices in the transverse plane of the tibia. The first measurement was performed after 5 days' recovery from surgery (week 0), and further measurements were performed at 1, 2, 3, and 5 weeks after the initial baseline scan. All scans were performed with an isotropic voxel size of 10.5 μm, 55 keV tube voltage, 109 μA tube current, and 200 ms integration time and captured 2,000 projections. Each scan delivered a radiation dose of 712.4 mGy (based on radiation probe inside a thin-walled polyetherimide cylinder), and a previous study determined that the effects of this radiation dose on bone architecture were small compared to changes due to estrogen deficiency [16]. Body mass of mice was determined at each scanning session.

At the end of the scanning protocol, all animals were killed and the right femur was harvested for in vitro micro-CT scanning (μCT 40, Scanco Medical) at a nominal isotropic resolution of 20 μm. All procedures were reviewed and approved by the University of Calgary Animal Care Committee.

Gray-scale CT images were segmented using a constrained gaussian filter (sigma = 1.2, support = 2) to remove noise, and a fixed threshold (25.5% of maximal gray-scale value) extracted the mineralized tissue structure. Morphological measurements included bone volume ratio (BV/TV), trabecular thickness/separation/number (Tb.Th, Tb.Sp, Tb.N), connectivity density (Conn.D), and structure-model index (SMI) calculated for each mouse at each time point (Image Processing Language, v5.00c; Scanco Medical). The region of interest for analysis of the in vivo data was the metaphyseal trabecular bone of the proximal tibia. User-defined contours were outlined on every tenth slice of a 150-slice region extending 1.575 mm distally from the growth plate, and a semiautomatic computer morphing algorithm was applied to the slices in between.

The distal femur at the study end point was analyzed in the metaphyseal region extending 100 slices (2 mm) proximally from the growth plate, and the midshaft region included 50 slices (1 mm) at the mid-diaphysis. An automated segmentation algorithm was used to extract the cortical and cancellous regions [18], and a morphological analysis (the same as the in vivo tibia analysis) was performed. At the femur midshaft, the analysis included measures of cross-sectional area of the medullary (MA), bone (BA), and total area (TA), as well as the cortical thickness (Ct.Th), polar moment of inertia (J), apparent density (D.App), and tissue density (D.Tiss) [13].

Statistics

The proximal tibia data were analyzed using a two-way repeated measures analysis of variance (ANOVA; SPSS, v14.0; SPSS, Inc., Chicago, IL) to examine interactions between time and treatment (OVX vs. sham) effect within each strain (C3H, B6, BALB) and interactions between genetic strain and OVX treatment effect. Differences between OVX and sham behavior at each time point were compared using unpaired Student's *t*-tests.

The distal and midshaft femur end point data were examined because these sites were not exposed to radiation during the in vivo experimental protocol and, thus, could confirm the results found in the tibia. These end point data were examined by a two-way ANOVA, again with factors being mouse strain and treatment (OVX vs. sham), and

Tukey post-hoc testing to compare OVX vs. sham animals within each mouse strain. ANOVA of the sham animals was performed to determine differences among inbred strains. The tests were two-tailed, and differences were considered significant at $P < 0.05$.

Finally, a regression was performed where the rate of bone loss (defined as the change per week over the first 3 weeks post-OVX) was the dependent variable and the baseline BV/TV was the independent variable. The regression was performed for all mouse strains pooled ($n = 23$) and for each of the three strains individually ($n = 7$ or 8).

Results

Morphological Longitudinal Changes in Response to OVX

Different skeletal responses to OVX were observed among the three mouse strains. Particularly, the parameters BV/TV, Tb.Th, Tb.N, and Conn.D were dependent on genetic strain, as indicated by a significant interaction ($P < 0.05$, F[4,48]) between strain and treatment effect. The average measurements of each parameter for OVX and sham groups of each strain at each time point are presented (Fig. 1, Table 1), and a significant time effect was found for all parameters measured and the three strains ($P < 0.005$, F[4,48]).

In the C3H strain, BV/TV was reduced by 45.1% in OVX animals 2 weeks after surgery. (The 45.1% change and all subsequent relative changes reported hereafter were significant to at least $P < 0.05$ and often to $P < 0.001$; details are available in Table 1.) A slower rate of loss was observed between weeks 2 and 5, resulting in 51.3% lower BV/TV at week 5 than at baseline. The average BV/TV at the end point for OVX C3H mice was 16.5 ± 5.8%. These mice displayed an 83.1% increase in Tb.Sp and a 42.9% reduction in Tb.N at week 5 compared to baseline. Bone loss was significantly greater in the OVX group ($P < 0.05$) than in the sham controls at every time point past baseline. Sham C3H mice showed <20% reduction in BV/TV throughout the 5-week protocol and displayed a 33.7% increase in Tb.Sp along with 21.7% reduction in Tb.N.

B6 mice had much lower BV/TV at baseline (~10% compared to ~35% in C3H). Over the course of the 5-week protocol, the OVX mice from the B6 strain lost 40.8% of their baseline bone volume (average BV/TV 6.2 ± 1.8% at the end point), but these losses were not significantly different from losses in the sham group at any time point. Likewise, although a 12.7% increase in Tb.Sp and a 32.4% reduction in Tb.N were observed in the OVX animals, these were not significantly different from similar patterns of loss observed in the sham animals and no statistical interaction was observed between the two groups for these parameters ($P > 0.2$).

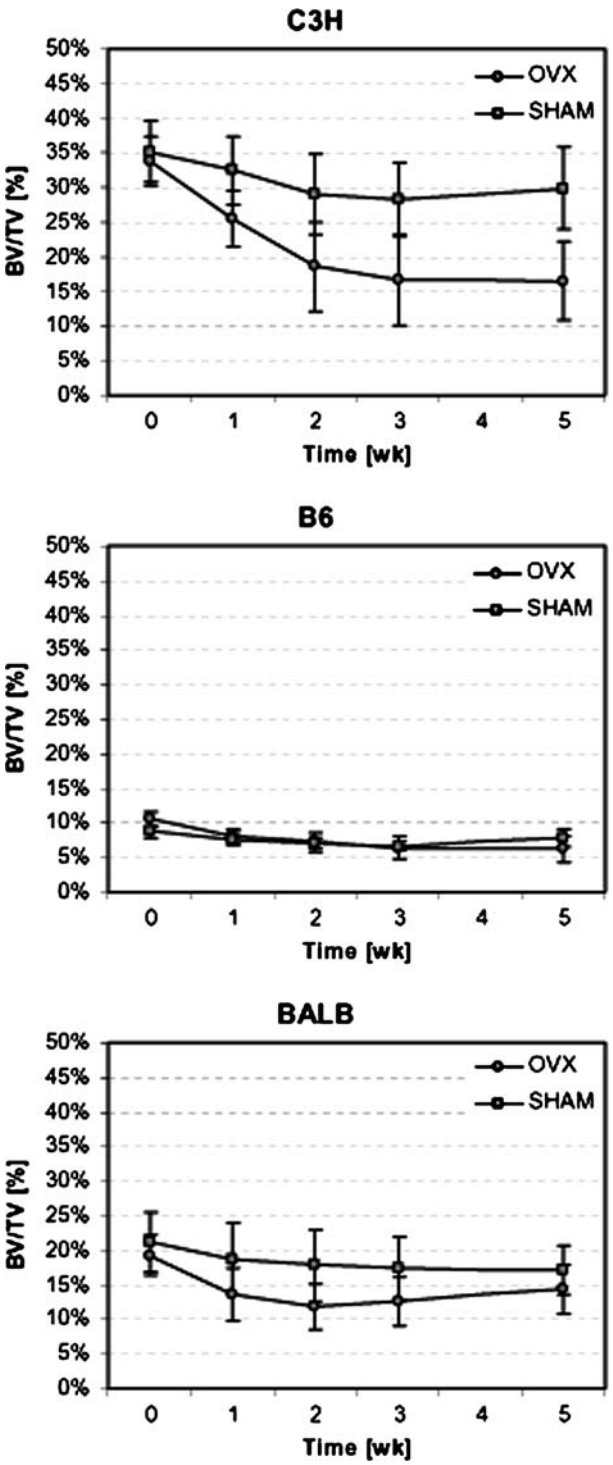

Fig. 1 Longitudinal changes in BV/TV for OVX and sham groups of each inbred mouse strain over the duration of the study. Group means and standard deviations are shown. OVX and sham surgeries were performed at 12 weeks of age, and baseline scan (week 0) was performed 5 days postsurgery

Table 1 Longitudinal morphology results by treatment group

	0 week	1 week	2 weeks	3 weeks	5 weeks
C3H					
BV/TV (%)					
OVX	33.9 ± 3.5	25.5 ± 4.0*	18.6 ± 6.4**	16.6 ± 6.6**	16.5 ± 5.8**
Sham	35.2 ± 4.4	32.5 ± 4.9*	29.0 ± 5.7*	28.3 ± 5.3**	29.9 ± 5.9**
Tb.Th (mm)					
OVX	0.077 ± 0.004	0.073 ± 0.005*	0.070 ± 0.007**	0.073 ± 0.008	0.075 ± 0.007
Sham	0.080 ± 0.004	0.080 ± 0.005	0.079 ± 0.005	0.082 ± 0.004	0.085 ± 0.007*
Tb.Sp (mm)					
OVX	0.188 ± 0.017	0.217 ± 0.013**	0.280 ± 0.042**	0.314 ± 0.052**	0.345 ± 0.052**
Sham	0.190 ± 0.011	0.203 ± 0.017*	0.228 ± 0.027*	0.238 ± 0.019**	0.254 ± 0.040*
Tb.N (1/mm)					
OVX	5.342 ± 0.335	4.638 ± 0.194**	3.670 ± 0.555**	3.299 ± 0.582**	3.052 ± 0.507**
Sham	5.368 ± 0.251	5.042 ± 0.343*	4.472 ± 0.415*	4.312 ± 0.315**	4.204 ± 0.639**
ConnD (1/mm^3)					
OVX	137.19 ± 14.78	104.08 ± 14.59**	54.97 ± 23.29**	44.21 ± 20.38**	41.20 ± 15.52**
Sham	140.29 ± 24.57	118.90 ± 20.14*	92.88 ± 18.13*	82.30 ± 14.55**	90.14 ± 20.40*
SMI (1)					
OVX	0.616 ± 0.347	1.396 ± 0.314*	1.810 ± 0.440**	2.021 ± 0.466**	1.838 ± 0.419**
Sham	0.541 ± 0.467	0.819 ± 0.555	0.983 ± 0.600*	1.002 ± 0.545*	0.856 ± 0.538
B6					
BV/TV (%)					
OVX	10.5 ± 1.2	8.1 ± 1.0*	7.3 ± 1.4**	6.4 ± 1.6**	6.2 ± 1.8**
Sham	8.8 ± 0.9	7.6 ± 0.9*	7.1 ± 0.8**	6.7 ± 0.5**	7.7 ± 1.3*
Tb.Th (mm)					
OVX	0.050 ± 0.002	0.049 ± 0.002	0.051 ± 0.002	0.051 ± 0.004	0.054 ± 0.004
Sham	0.047 ± 0.002	0.049 ± 0.002*	0.051 ± 0.002*	0.052 ± 0.002*	0.057 ± 0.004**
Tb.Sp (mm)					
OVX	0.316 ± 0.030	0.364 ± 0.044*	0.410 ± 0.029**	0.433 ± 0.057*	0.477 ± 0.091*
Sham	0.336 ± 0.027	0.396 ± 0.029*	0.429 ± 0.059*	0.441 ± 0.027**	0.439 ± 0.038*
Tb.N (1/mm)					
OVX	3.246 ± 0.293	2.797 ± 0.286**	2.477 ± 0.200**	2.382 ± 0.279**	2.194 ± 0.403**
Sham	3.047 ± 0.243	2.591 ± 0.173*	2.421 ± 0.262*	2.312 ± 0.128**	2.358 ± 0.181*
ConnD (1/mm^3)					
OVX	53.43 ± 13.78	31.87 ± 10.95*	28.63 ± 12.16*	21.97 ± 9.91**	19.56 ± 9.48**
Sham	43.04 ± 11.27	31.17 ± 7.59*	25.43 ± 8.16*	22.63 ± 5.61**	25.30 ± 6.11*
SMI (1)					
OVX	2.435 ± 0.080	2.606 ± 0.141*	2.665 ± 0.231*	2.779 ± 0.183*	2.667 ± 0.162*
Sham	2.494 ± 0.145	2.530 ± 0.150	2.532 ± 0.213	2.539 ± 0.154	2.264 ± 0.256*
BALB					
BV/TV (%)					
OVX	19.2 ± 2.9	13.6 ± 3.7**	11.8 ± 3.3**	12.7 ± 3.6**	14.4 ± 3.5*
Sham	21.1 ± 4.3	18.8 ± 5.2*	17.8 ± 5.1**	17.4 ± 4.6**	17.1 ± 3.6**
Tb.Th (mm)					
OVX	0.060 ± 0.003	0.056 ± 0.005*	0.059 ± 0.004	0.062 ± 0.004	0.066 ± 0.006*
Sham	0.061 ± 0.004	0.061 ± 0.005	0.064 ± 0.005*	0.065 ± 0.004*	0.067 ± 0.003**
Tb.Sp (mm)					
OVX	0.218 ± 0.015	0.269 ± 0.028**	0.309 ± 0.043**	0.325 ± 0.056**	0.332 ± 0.079*
Sham	0.209 ± 0.026	0.226 ± 0.033*	0.247 ± 0.035**	0.256 ± 0.040**	0.285 ± 0.043**

Table 1 Longitudinal morphology results by treatment group

	0 week	1 week	2 weeks	3 weeks	5 weeks
Tb.N (1/mm)					
OVX	4.642 ± 0.269	3.777 ± 0.403**	3.320 ± 0.416**	3.201 ± 0.490**	3.201 ± 0.561**
Sham	4.857 ± 0.557	4.504 ± 0.614*	4.091 ± 0.530**	3.987 ± 0.597**	3.653 ± 0.487**
ConnD ($1/mm^3$)					
OVX	107.63 ± 22.00	61.67 ± 20.19**	38.99 ± 18.22**	46.75 ± 9.65**	52.26 ± 20.87**
Sham	118.98 ± 23.16	92.54 ± 35.41**	69.53 ± 24.50**	68.97 ± 27.45**	55.78 ± 15.90**
SMI (1)					
OVX	1.887 ± 0.268	2.162 ± 0.348*	2.279 ± 0.299*	2.180 ± 0.258*	2.003 ± 0.268
Sham	1.749 ± 0.310	1.919 ± 0.333	1.875 ± 0.438	1.870 ± 0.327*	1.631 ± 0.287

Measurements for each time point are group averages (mean ± SD), and significant changes with respect to baseline are indicated (* $P < 0.05$, ** $P < 0.001$)

BALB mice had moderate BV/TV levels at baseline (~20%), which were reduced in the OVX animals by 29.3% at week 1 and 38.6% at week 2. However, between weeks 2 and 3 the mean change showed a recovery, and by week 5 all BALB mice had higher BV/TV levels than they had at week 2. The average BV/TV for OVX BALB mice at week 5 was 14.4 ± 3.5%. In OVX BALB animals, Tb.Sp increased by 13.0% at week 5 compared to baseline, while Tb.N declined by 31.0%. Bone losses in the sham BALB mice were steady and not as severe as those observed within the first 2 weeks for the OVX animals. At week 5, shams had lost 19.0% of their baseline BV/TV, with a 9.1% increase in Tb.Sp and a 24.8% reduction in Tb.N. For BV/TV, Tb.Sp, and Tb.N, the changes in OVX were significantly different ($P < 0.05$) than shams at weeks 1, 2, and 3 only, with recovery between weeks 3 and 5, leading to no significant difference between OVX and shams at the final time point.

Tb.Th was observed to decrease in OVX mice relative to shams for both C3H (11.8% decrease at week 5, $P < 0.05$) and BALB (7.9% decrease at week 3, $P < 0.05$). Tb.Th in the OVX B6 group did not change over time with respect to baseline, although the sham B6 mice showed a Tb.Th increase of 16.3% between baseline and week 5.

Conn.D decreased over time for all groups, and for C3H and BALB these losses were significantly more pronounced in the OVX animals. The OVX C3H mice lost 60% of their connectivity by week 2 and 70% by week 5. The OVX BALB mice lost 64% by week 2 and recovered slightly toward week 5. The OVX B6 mice lost 63% of their connectivity by week 5, but this was not significantly different from the 41% loss in the sham animals.

All OVX groups showed progression toward more rod-like trabecular structures over time relative to shams, as indicated by increasing SMI. The OVX C3H mice had significantly higher SMI relative to shams from week 1 onward, increasing from 0.6 (plate-like) at baseline to 1.8 (more rod-like) at week 5, with a maximum of 2.0 at week 3. OVX BALB mice were significantly different from shams starting at week 2, with an increase from 1.9 at baseline to 2.3 at week 2 and a return to 2.0 at week 5. The OVX B6 were significantly different from shams from week 3 onward, increasing from a baseline SMI value of 2.44 to 2.67 at week 5, with a peak increase to 2.78 at week 3.

In all three strains of mice, both the OVX and sham groups increased in body mass from baseline to week 5 ($P < 0.01$, Table 2).

Femur Metaphyseal and Midshaft Response to OVX at End Point

The changes to the distal femur metaphyseal region for all three strains of mice followed the same trends as observed from in vivo data at the proximal tibia site (Table 3).

Table 2 Body mass for the three inbred strains of mice at baseline (week 0) and at the end point (week 5): means and SD (in parentheses) are shown for each group

	C3H		B6		BALB	
Body mass (g)	OVX ($n = 7$)	Sham ($n = 7$)	OVX ($n = 8$)	Sham ($n = 7$)	OVX ($n = 8$)	Sham ($n = 8$)
Baseline (week 0)	20.1 (2.5)	20.3 (2.0)	19.7 (1.3)	19.7 (1.3)	20.9 (1.2)	21.7 (1.7)
End point (week 5)	26.2 (3.6)*	23.9 (3.1)*	24.2 (3.7)*	22.1 (2.2)*	23.7 (1.5)*	23.8 (2.4)*

Significant difference between end point and baseline (* $P < 0.01$, paired t-test)

Table 3 Morphometric indices of the metaphyseal region of the distal femur and the femur midshaft at 5 weeks for OVX and sham animals: means and SD (in parentheses) are shown for each group

	C3H		B6		BALB	
	OVX ($n = 7$)	Sham ($n = 7$)	OVX ($n = 8$)	Sham ($n = 7$)	OVX ($n = 8$)	Sham ($n = 8$)
Femur distal						
BV/TV (%)	19.2 (6.6)*	31.8 (4.2)^{b,c}	3.7 (1.2)	4.3 (1.1)^{a,c}	13.6 (5.1)*	21.0 (7.5)^{a,b}
Tb.N (mm^{-1})	3.2 (0.7)*	4.0 (0.3)^{b}	2.8 (0.5)	3.0 (0.3)^{a,c}	3.6 (0.5)*	4.2 (0.5)^{b}
Tb.Th (mm)	0.09 (0.01)*	0.10 (0.00)^{b,c}	0.05 (0.01)	0.05 (0.01)^{a,c}	0.07 (0.01)	0.07 (0.01)^{a,b}
Tb.Sp (mm)	0.33 (0.10)*	0.24 (0.03)^{b}	0.37 (0.07)	0.34 (0.03)^{a,c}	0.29 (0.05)*	0.24 (0.04)^{b}
Ct.Th (mm)	0.13 (0.02)	0.14 (0.02)^{b,c}	0.06 (0.02)	0.05 (0.01)^{a,c}	0.07 (0.01)	0.08 (0.01)^{a,b}
Conn.D (mm^{-3})	31.3 (12.9)*	59.1 (12.3)^{b}	5.0 (3.6)	5.0 (3.2)^{a,c}	41.2 (19.4)	55.4 (23.5)^{b}
SMI (−)	2.33 (0.21)*	1.42 (0.44)^{b}	4.16 (0.27)	4.21 (0.40)^{a,c}	2.80 (0.43)*	2.10 (0.72)^{b}
D.App (mg HA/cm^3)	208 (53)*	292 (23)^{b,c}	95 (13)	106 (7)^{a,c}	166 (41)*	217 (40)^{a,b}
Femur midshaft						
TA (mm^2)	1.41 (0.07)	1.37 (0.07)^{b,c}	1.63 (0.08)	1.59 (0.10)^{a}	1.50 (0.10)	1.53 (0.08)^{a}
BA (mm^2)	1.17 (0.05)	1.14 (0.07)^{b,c}	0.81 (0.02)	0.81 (0.05)^{a,c}	0.98 (0.05)	0.99 (0.05)^{a,b}
MA (mm^2)	0.24 (0.04)	0.24 (0.02)^{b,c}	0.82 (0.06)	0.78 (0.05)^{a,c}	0.52 (0.07)	0.54 (0.04)^{a,b}
BA/TA (%)	83.2 (2.2)	82.8 (1.2)^{b,c}	49.5 (1.4)*	51.0 (0.5)^{a,c}	65.3 (2.6)	64.8 (1.1)^{a,b}
Ct.Th (mm)	0.38 (0.02)	0.37 (0.02)^{b,c}	0.20 (0.01)	0.20 (0.00)^{a,c}	0.27 (0.01)	0.27 (0.01)^{a,b}
J (mm^4)	328 (33)	313 (33)	352 (32)	341 (38)	340 (42)	355 (34)
D.App (mg HA/cm^3)	803 (35)	788 (16)^{b,c}	447 (12)*	465 (8)^{a,c}	624 (31)	620 (11)^{a,b}
D.Tiss (mg HA/cm^3)	950 (34)	935 (13)^{b,c}	805 (13)	813 (12)^{a,c}	893 (20)	895 (11)^{a,b}

Significant difference between OVX and sham (* $P < 0.05$). Significantly different ($P < 0.05$) from [a] C3H, [b] B6 and [c] BALB

However, the statistical power of the end point measurements (cross-sectional statistical analysis) was less than the in vivo repeated measures assessment of the proximal tibia. This was reflected in the lack of significance of the morphological changes in the OVX B6 mice in particular, as well as some of the parameters for the OVX BALB mice. Conversely, in the OVX C3H mice, which had the greatest absolute magnitude of change, all morphological parameters (with the exception of Ct.Th) were significantly different between the OVX and sham controls.

At the femur midshaft, no significant effects of OVX were detected for all three strains of mice with the exception of B6 mice, which had a significant reduction in D.App (and corresponding BA/TA) due to OVX.

Rate of Loss

Rate of bone loss for each OVX animal, defined as the slope of the linear line that best fit the animal's BV/TV data over weeks 0, 1, 2, and 3, was found to be dependent on the baseline BV/TV when all OVX mice were pooled, resulting in a Pearson correlation of $R = 0.822$ ($n = 23$, $P < 0.001$). The animals with higher baseline BV/TV lost more bone in the same amount of time as animals with lower baseline BV/TV (Fig. 2). When each strain was considered independently, no significant correlations were found (C3H $n = 7$, $R = 0.291$, $P = 0.526$; B6 $n = 8$, $R = 0.574$, $P = 0.137$; BALB $n = 8$, $R = 0.435$, $P = 0.282$), although it should be noted that group sizes were small ($n = 7$ or 8) for each individual mouse strain. The variation in response to OVX was higher in the strains with higher quantity of baseline bone.

Discussion

This study longitudinally tracked the skeletal response to OVX at the proximal tibia in three inbred strains of mice over a 5-week period and demonstrated distinct patterns of loss over time for each strain. The magnitude of change due to OVX differed among the three strains, and the rate of change was largely explained by the baseline bone volume ratio of each mouse strain. Furthermore, after the skeletal changes had become more stable at the end of the 5-week protocol, differences in bone quantity remained for each strain, and this was true at both the tibia and femur measurement sites.

It should be noted that at the start of the study the mice were 12 weeks old and had only recently reached skeletal maturity; therefore, the longitudinal changes may differ if older mice are studied. Also, we did not verify OVX by measuring uterine weight post mortem, as has been done in

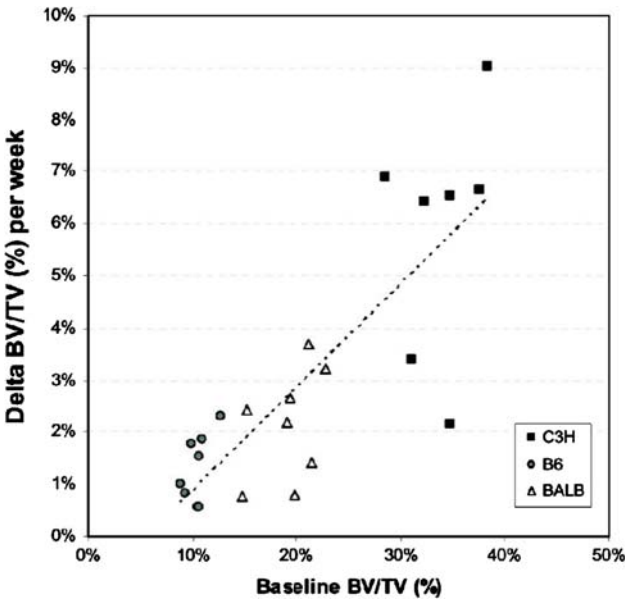

Fig. 2 Regression between baseline BV/TV and rate of OVX bone loss between weeks 0 and 3 for the three inbred mouse strains

previous studies [13, 14], although we are confident that the operation was successful, as reflected in the clear trends in the morphological data at the tibia and verified by the femur sites which also exhibited significant differences between OVX and sham animals for all three strains. The in vivo protocol results in repeated radiation doses, and although no effects have been detected in rats [16, 19], there is evidence of small bone effects in mice [16]. Of the three strains, the C3H mice exhibited the strongest effects, but even these were small (3% reduction in BV/TV [16] compared to the total change of 17% BV/TV due to OVX). The estrogen-related changes are dominant, and trends in the proximal tibia were consistent with trends at the non-irradiated femur sites. Furthermore, it is unlikely that interaction between OVX and radiation (e.g., exaggeration of bone loss) occurs because the absolute bone changes we measured are very close in magnitude to those reported by others [13], where no radiation was present. Nevertheless, future in vivo mouse studies should use the lowest resolution possible and reduce scanning frequency to minimize radiation.

The sham control mice of all three strains exhibited a significant reduction in cancellous bone at the proximal tibia throughout the duration of the in vivo study (BV/TV, $P < 0.05$), and this may seem to be counterintuitive because these were young, growing mice [9]. However, our results showing decreases with age are consistent with previous studies that showed a reduction in cancellous bone, also at the proximal tibia, in male B6 mice beginning at 6 weeks of age [20]. The early reduction was confirmed by others [21] and shown to be even more pronounced in female mice. Although Beamer and colleagues [9] showed that peak bone mass occurs at approximately 16 weeks of age, those data were based on bone density measurements that combined cancellous and cortical compartments. The whole bone density, as noted recently by Glatt and colleagues [21], may represent the thickening cortex with age that overshadows early onset of cancellous bone decreases. Thus, our finding of increased body mass from age 12 to 17 weeks in conjunction with decreased cancellous bone is consistent with previous findings and reinforces the notion that body mass is not a good indicator of cancellous bone quantity and must be carefully considered in the mouse OVX model of osteoporosis.

The morphological response to OVX differed among the inbred strains, and the patterns of bone loss observed here agree well with OVX responses observed in these same strains of mice in a recent cross-sectional ex vivo study by Bouxsein and colleagues [13]. In the current study, and consistent with the previous one [13], C3H mice displayed the highest rates and extent of bone loss after OVX ($\sim$50% bone loss relative to baseline, $\sim$45% reduction relative to sham), while OVX-operated BALB mice also incurred large losses ($\sim$40% bone loss relative to baseline, $\sim$30% reduction relative to sham). Our result that OVX B6 mice did not show significantly greater reductions in BV/TV than their sham-operated controls is also consistent. In contrast to previous results [13], we found greater increases in Tb.Sp in the OVX C3H and BALB mice and significant declines in Tb.N for C3H (up to 27.4% reduction at week 5, $P < 0.05$) and BALB (up to 19.7% reduction at week 3, $P < 0.05$). It is possible that the in vivo nature of the current study was more sensitive to these changes or that the changes are related to our use of younger mice.

The longitudinal patterns of bone changes measured in vivo provide insight into the time-sensitive responses to OVX in the three strains. For the C3H mice, we can observe that the highest rates of OVX-induced bone loss occur between week 0 and week 2, with an asymptotic "leveling-out" occurring in all animals between week 3 and week 5 where no further bone loss was detected. Likewise, bone loss in B6 mice was greatest between week 0 and week 1, with steady declines through week 2 and week 3 and only small further reductions between week 3 and week 5. Examining each BALB mouse in vivo over the study period revealed a maximal extent of bone loss occurring at week 2, after which a recovery trend was observed in all animals of that group between week 2 and week 5. Each strain behaved differently, and there was not a common "low point" shared between the strains. BV/TV in C3H mice reached a minimum near 16%, while BALB mice dropped to 12% before recovering to 14%. Bone loss in both of the higher bone mass strains (C3H and BALB) stopped short of reaching the lower BV/TV levels of B6

mice, whose BV/TV dropped from 10% to 6% before leveling out. This difference between strains occurred at the proximal tibia as well as the distal femur.

The regression between rate of bone loss and baseline BV/TV indicates that higher baseline BV/TV does not necessarily offer protection against osteopenic changes. Despite having the highest initial BV/TV, C3H mice also incurred the highest rates of bone loss, both absolute ($BV/TV_{week\ 3} - BV/TV_{week\ 0}$) and relative (absolute/$BV/TV_{week\ 0}$). Since OVX leads to increased rates of bone turnover [22–24], it is reasonable that areas with high volumes of bone would see high volume losses. However, although the relative losses were substantial for all strains (50% for C3H, 40% for B6, 38% for BALB), the absence of a common low point means the strains with higher initial BV/TV are left with more bone after skeletal homeostasis post-OVX. Additionally, although the relation between rate of loss and baseline bone volume ratio is strong ($R = 0.82$), it remains to be determined whether augmenting bone (i.e., mechanical intervention or pharmaceutical therapy) could protect against loss *within* a particular mouse strain. Nevertheless, the differences between the three genetic strains tested here support the hypothesis that OVX bone loss is in part genetically regulated.

The BALB strain was the only one in which a recovery effect was observed after initial reduction of bone volume. On average, OVX-operated BALB mice regained 42% of their lost bone. The mechanism behind this recovery is unclear; however, the results show that the increases in Tb.Sp and decreases in Tb.N reached an asymptote after week 3, while Tb.Th steadily increased from week 1 onward. A possible explanation is that the unresorbed trabeculae thickened over time in response to increased mechanical loading. The apparent recovery could also be related to higher activity levels in BALB mice. The positive effect of mechanical stimuli and exercise on bone strength and structure recovery has been observed in rats and mice [25–27], and although activity levels were not specifically monitored here, BALB mice showed the least body mass increase over the study period ($\sim$50% less mass gain than other strains for OVX groups, Table 2), which, in addition to the qualitative observation that BALB mice were more energetic than C3H and B6 during the study, could be indicative of higher overall activity levels.

Examining the in vivo morphological data offers insight into how OVX-induced bone loss is manifested in the trabecular bone structure. C3H mice incurred significant increases in Tb.Sp and decreases in Tb.N, while Tb.Th was relatively unaffected. Conn.D also decreased significantly between baseline and week 5. B6 mice followed a similar pattern but with lesser magnitude. BALB mice also increased Tb.Sp, decreased Tb.N, and decreased Conn.D, while Tb.Th steadily increased. These trends may indicate losses of connectivity as a result of resorbed trabeculae, as opposed to gradual thinning of the entire structure. These trends can be verified by examining three-dimensional images from each time point for the individual animals (Fig. 3), where images from representative mice (median of each group) have been aligned with three-dimensional image registration techniques [28]. Specific structures can be identified and followed between time points. For example, structures present near the middle of the metaphysis at baseline have been resorbed at the later time points, while thick plate-like structures can be seen to perforate into multiple rod-like structures. These patterns

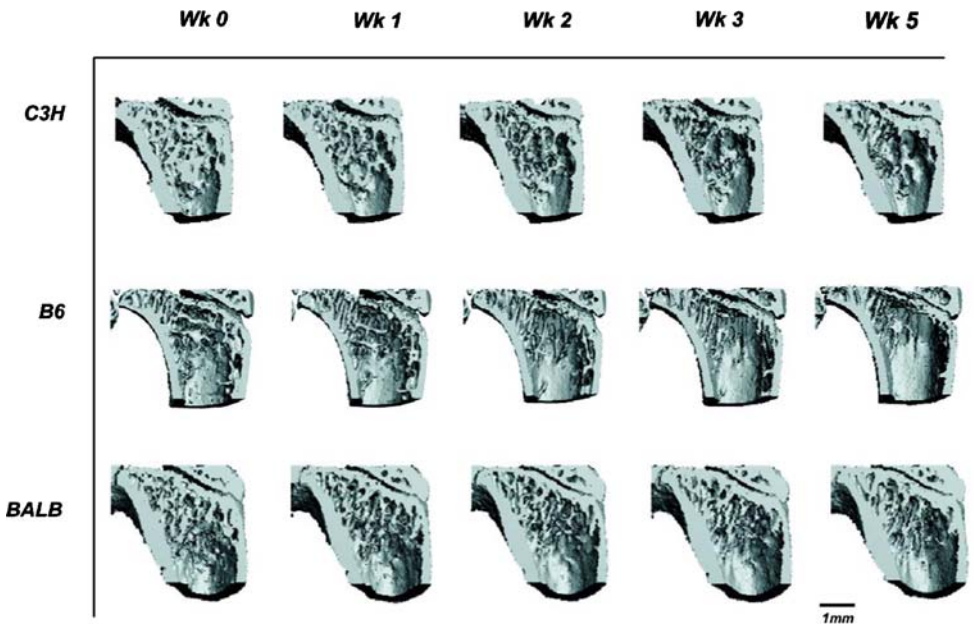

Fig. 3 Longitudinal three-dimensional in vivo images of three OVX animals representative of each inbred strain. Specific structures can be identified and qualitatively compared between time points. Representative animals from each group were selected based on having the median baseline BV/TV within their respective group

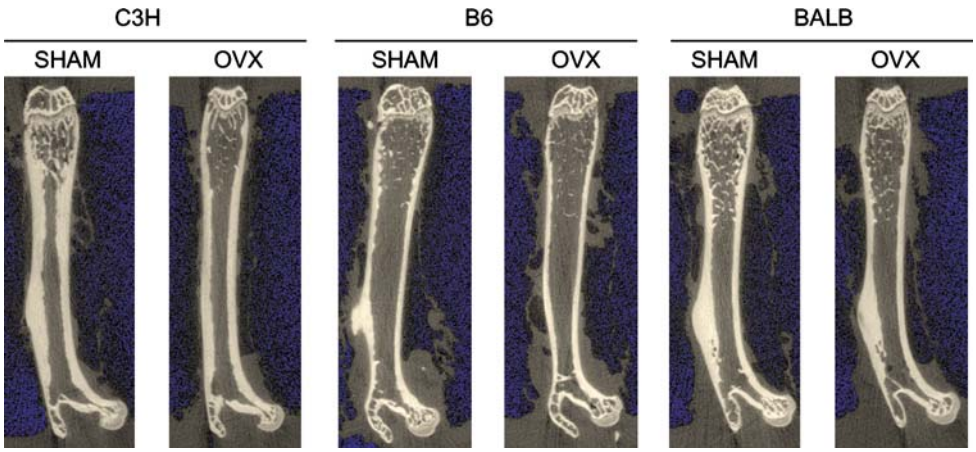

Fig. 4 End point scans of a representative OVX and sham femur from each of the three inbred mouse strains at week 5, illustrating fundamental differences in bone architecture

can be observed to different degrees in each of the strains and illustrate that, although the morphology after OVX differs between strains, there are commonalities in the patterns of bone loss.

The use of B6 has been questioned as an appropriate model for osteoporosis research due to its insensitivity to OVX, among other reasons [14]; and this is confirmed by our results here because the majority of morphological measures in both the tibia and femur were not statistically significant 5 weeks after OVX. The primary issue is that the proximal tibia and femur have very little cancellous bone, which makes it difficult to observe significant skeletal responses due to OVX. This can be clearly seen in the representative mice from each group (Figs. 3 and 4). Although the relative difference in bone volume ratio of OVX B6 compared to shams was large (40.8% decrease), it is important to note that the change was not significant compared to the sham animals and the end point absolute bone volume ratio was very low (6.2%). Reporting relative changes overstates the effect of OVX in this animal model. On the other hand, the higher bone mass mice, BALB and C3H, were significantly changed due to the OVX operation at the proximal tibia (which is a convenient skeletal site to measure by in vivo micro-CT), and these strains may be more appropriate for research into estrogen-deficient bone loss.

In conclusion, the skeletal response to OVX was different between inbred strains of mice, supporting the hypothesis that estrogen deficiency–related bone loss is in part genetically regulated; and this is also reflected in the significant regression between rate of bone loss and baseline bone. Strains with higher initial bone volume had higher rates of bone loss but also maintain higher levels of BV/TV once an asymptote has been reached (stabilized skeletal changes). There is not a common low point independent of inbred strain. Bone loss appears to be manifested through resorption of trabecular elements, particularly those farthest from the cortical wall. The in vivo nature of the measurements performed here offers new insight into the time-based behavior of bone, and further investigations into treatments and preventive measures against bone loss are warranted.

Acknowledgements This work was supported by grants from the Natural Sciences and Engineering Research Council of Canada, the Canadian Institutes of Health Research, the Canada Foundation for Innovation, the Alberta Heritage Foundation for Medical Research, and the Alberta Ingenuity Fund.

References

1. World Health Organization (1994) Assessment of fracture risk and its application to screening for postmenopausal osteoporosis. WHO, Geneva, pp 1–129
2. Melton LJ 3rd, Chrischilles EA, Cooper C, Lane AW, Riggs BL (1992) Perspective. How many women have osteoporosis? J Bone Miner Res 7:1005–1010
3. Ray NF, Chan JK, Thamer M, Melton LJ 3rd (1997) Medical expenditures for the treatment of osteoporotic fractures in the United States in 1995: report from the National Osteoporosis Foundation. J Bone Miner Res 12:24–35
4. Harris S, Dawson-Hughes B (1992) Rates of change in bone mineral density of the spine, heel, femoral neck and radius in healthy postmenopausal women. Bone Miner 17:87–95
5. Radspieler H, Dambacher MA, Kissling R, Neff M (2000) Is the amount of trabecular bone-loss dependent on bone mineral density? A study performed by three centres of osteoporosis using high resolution peripheral quantitative computed tomography. Eur J Med Res 5:32–39
6. Pouilles JM, Tremollieres F, Ribot C (1995) Effect of menopause on femoral and vertebral bone loss. J Bone Miner Res 10:1531–1536
7. Karasik D, Ginsburg E, Livshits G, Pavlovsky O, Kobyliansky E (2000) Evidence of major gene control of cortical bone loss in humans. Genet Epidemiol 19:410–421
8. Peacock M, Turner CH, Econs MJ, Foroud T (2002) Genetics of osteoporosis. Endocr Rev 23:303–326
9. Beamer WG, Donahue LR, Rosen CJ, Baylink DJ (1996) Genetic variability in adult bone density among inbred strains of mice. Bone 18:397–403
10. Turner CH, Hsieh YF, Müller R, Bouxsein ML, Baylink DJ, Rosen CJ, Grynpas MD, Donahue LR, Beamer WG (2000)

Genetic regulation of cortical and trabecular bone strength and microstructure in inbred strains of mice. J Bone Miner Res 15:1126–1131
11. Turner CH, Hsieh YF, Müller R, Bouxsein ML, Rosen CJ, McCrann ME, Donahue LR, Beamer WG (2001) Variation in bone biomechanical properties, microstructure, and density in BXH recombinant inbred mice. J Bone Miner Res 16:206–213
12. Alexander JM, Bab I, Fish S, Müller R, Uchiyama T, Gronowicz G, Nahounou M, Zhao Q, White DW, Chorev M, Gazit D, Rosenblatt M (2001) Human parathyroid hormone 1–34 reverses bone loss in ovariectomized mice. J Bone Miner Res 16:1665–1673
13. Bouxsein ML, Myers KS, Shultz KL, Donahue LR, Rosen CJ, Beamer WG (2005) Ovariectomy-induced bone loss varies among inbred strains of mice. J Bone Miner Res 20:1085–1092
14. Iwaniec UT, Yuan D, Power RA, Wronski TJ (2006) Strain-dependent variations in the response of cancellous bone to ovariectomy in mice. J Bone Miner Res 21:1068–1074
15. Boyd SK, Davison P, Müller R, Gasser JA (2006) Monitoring individual morphological changes over time in ovariectomized rats by in vivo micro-computed tomography. Bone 39:854–862
16. Klinck RJ, Campbell GM, Boyd SK (2008) Radiation effects on bone architecture in mice and rats resulting from in vivo micro-computed tomography scanning. Med Eng Phys (in press). doi: 10.1016/j.medengphy.2007.11.004
17. Brouwers JE, van Rietbergen B, Huiskes R (2007) No effects of in vivo micro-CT radiation on structural parameters and bone marrow cells in proximal tibia of Wistar rats detected after eight weekly scans. J Orthop Res 25:1325–1332
18. Buie HR, Campbell GM, Klinck RJ, MacNeil JA, Boyd SK (2007) Automatic segmentation based on a dual threshold technique for in vivo micro-CT bone analysis. Bone 41:505–515
19. Brouwers JE, van Rietbergen B, Huiskes R (2007) No effects of in vivo micro-CT radiation on structural parameters and bone marrow cells in proximal tibia of Wistar rats detected after eight weekly scans. J Orthop Res 25:1325–1332
20. Halloran BP, Ferguson VL, Simske SJ, Burghardt A, Venton LL, Majumdar S (2002) Changes in bone structure and mass with advancing age in the male C57BL/6J mouse. J Bone Miner Res 17:1044–1050
21. Glatt V, Canalis E, Stadmeyer L, Bouxsein ML (2007) Age-related changes in trabecular architecture differ in female and male C57BL/6J mice. J Bone Miner Res 22:1197–1207
22. David V, Laroche N, Boudignon B, Lafage-Proust MH, Alexandre C, Rüegsegger P, Vico L (2003) Noninvasive in vivo monitoring of bone architecture alterations in hindlimb-unloaded female rats using novel three-dimensional microcomputed tomography. J Bone Miner Res 18:1622–1631
23. Sims NA, Morris HA, Moore RJ, Durbridge TC (1996) Increased bone resorption precedes increased bone formation in the ovariectomized rat. Calcif Tissue Int 59:121–127
24. Kalu DN, Liu CC, Hardin RR, Hollis BW (1989) The aged rat model of ovarian hormone deficiency bone loss. Endocrinology 124:7–16
25. Wronski TJ, Cintron M, Dann LM (1988) Temporal relationship between bone loss and increased bone turnover in ovariectomized rats. Calcif Tissue Int 43:179–183
26. Honda A, Umemura Y, Nagasawa S (2001) Effect of high-impact and low-repetition training on bones in ovariectomized rats. J Bone Miner Res 16:1688–1693
27. Honda A, Sogo N, Nagasawa S, Shimizu T, Umemura Y (2003) High-impact exercise strengthens bone in osteopenic ovariectomized rats with the same outcome as sham rats. J Appl Physiol 95:1032–1037
28. Boyd SK, Moser S, Kuhn M, Klinck RJ, Krauze PL, Müller R, Gasser JA (2006) Evaluation of three-dimensional image registration methodologies for in vivo micro-computed tomography. Ann Biomed Eng 34:1587–1599